Multiple Nonlinear Harmonic Oscillator-Based Frequency Estimation for Distorted Grid Voltage

Hafiz Ahmed, Michael Bierhoff and Mohamed Benbouzid

https://dx.doi.org/10.1109/TIM.2019.2931065

ISSN 0018-9456
ESSN 1557-9662

Publisher: IEEE

Multiple Nonlinear Harmonic Oscillator-Based Frequency Estimation for Distorted Grid Voltage

Hafiz Ahmed, *Member, IEEE,* Michael Bierhoff, *Member, IEEE,* and Mohamed Benbouzid, *Senior Member, IEEE*

***Abstract*—In the presence of nonlinear loads and various disturbances, harmonics and DC bias may corrupt the grid voltage signal leading to distorted grid. Frequency estimation of distorted grid signal is a challenging issue. In this paper, multiresonant nonlinear harmonic oscillators based frequency estimation technique is reported for distorted power grid. The proposed approach has also been applied for detecting the sequences of unbalanced grid. In the proposed approach, a nonlinear harmonic oscillator is used as the proxy of the grid signal. Then using the frequency-locked loop, an adaptive approach is proposed to estimate the frequency and other parameters (sequences) in the presence of harmonics and DC component. Local stability analysis and parameter tuning are provided. Comparative experimental results are provided with two other nonlinear state of the art techniques. Experimental results demonstrated the suitability of the proposed technique.**

***Index Terms*—Frequency estimation, three-phase sequence detection, frequency-locked loop, unbalanced grid voltage**

I. Introduction

Phase, frequency and amplitude characterize the single-phase grid voltage signal while symmetric components characterize the three-phase grid voltage signal. They are useful in numerous control and monitoring applications related to power system. They are used in the control of grid connected power converters [1]–[3], active power filter [4]–[6], bidirectional electric vehicle charger [7], uninterrupted power supply [8], distributed generation systems [9], power grid monitoring [10] *etc.* The importance of fast and accurate estimation of grid voltage parameters and sequences can be easily seen from the list of applications. As a result, numerous results are reported in the literature to estimate the parameters and sequences of the grid voltage signal.

Some of the popular techniques proposed in the literature are discrete Fourier transform (DFT) [11], [12], neural network [13], various variants of least-square (weighted, recursive *etc.*) [14]–[16] techniques, linear observer based techniques (Luenberger observer, Kalman filter *etc.*) [17]–[19], various variants of phase-locked loop (PLL) [20]–[26], frequency-locked loop including second order generalized integrator [1], [27], adaptive notch filter (ANF) [28]–[30], statistical techniques [10], [31]–[33], limit cycle oscillator [34]–[36] *etc.* All these techniques have their own merits and demerits.

H. Ahmed is with the School of Mechanical, Aerospace and Automotive Engineering, Coventry University, The Futures Institute, Coventry CV1 2TL, United Kingdom. Corresponding author: H. Ahmed, E-mail: hafiz.h.ahmed@ieee.org, Tel: +44-2-477650023.

M. Bierhoff is with the Faculty of Electrical Engineering, University of Applied Sciences 18435, Stralsund, Germany.

M. Benbouzid is with the University of Brest, FRE CNRS 3744 IRDL - Institut de Recherche Dupuy de Lome, Brest, France. He is also with the Shanghai Maritime University, 201306 Shanghai, China.

Various variants of DFT based techniques [37] are using frequency domain approach. Since grid voltage signal has clearly distinguishable frequency feature, DFT based techniques are very useful. However, in the presence of harmonics, data window size increases for DFT based techniques which increases the computational cost. Moreover spectral leakage and accumulation error are reported in the literature for DFT based techniques. Regression based techniques like various variants of least-square [14]–[16] can efficiently estimate the parameters however they are computationally expensive as online matrix inversion is needed. Moreover, time-varying nature of the frequency can not be accommodated directly into least-square based techniques. Indirect way like using forgetting factors may solve that problem. Kalman filter [19] based approach can directly take into account the time varying nature of the frequency parameters. However, it uses a predictor-corrector structure that increases the computational complexity. Moreover, tuning of the parameters are mostly heuristics. Linear observer *e.g.* Luenberger observer [18] can solve these problems. However, the performance degrades significantly in the presence of harmonics and/or DC bias.

Out of all the techniques mentioned at the beginning, PLL and its various variants are the most popular techniques in the literature. They are time tested, widely used in numerous technical areas, simple structure, easy to tune and implement in an wide range of embedded hardwares. However PLLs performance suffers in distorted grid conditions. Moreover, fast dynamic response comes at a cost of disturbance rejection capability. To overcome the limitation of standard PLL, many modifications have been proposed in the literature e.g. using moving average filtering [38], low-pass notch filter [39], various variants of delayed signal cancellation [40], [41] to name a few. These modifications improved the performance of standard PLL in the presence of distorted grid condition. However, since the frequency is estimated through a proportional-integral (PI) type low-pass loop filter, the dynamic response relies heavily on the tuning of the loop-filter. Fast dynamic response is generally obtained through a second-order response type tuning which introduces overshoot in the frequency estimation loop.

Enhanced PLL (EPLL) [21] is another type of PLL that uses a nonlinear structure. Later on, EPLL has been extended for distorted grid conditions including harmonics and DC component [42], [43]. However, as suggested in [44], EPLLs dynamic response is slow and not suitable for application where fast convergence is required.

In recent times, two nonlinear techniques emerged as a strong competitor to PLL. They are second order generalized integrator - frequency-locked loop (SOGI-FLL) [27] and adaptive notch filter (ANF) [30]. Various variants of these techniques are also reported in the literature. SOGI-FLL and ANF use linear harmonic oscillator. Although the overall structure is nonlinear but the principal component is linear. As a result, they suffer from voltage swell and sags. Nonlinear oscillators are used in [34]. However, this technique is not immune to DC bias. Moreover, the presence of harmonics or any change of the amplitude from the nominal value will give rise to steady-state error.

To overcome the issues related to nonlinear oscillator based approach, a different kind of oscillator *i.e.* circular limit cycle oscillator (CLO) is used in [35]. The oscillator structure of CLO is computationally simpler than that of [34]. Although CLO can handle DC offset disturbance but details are missing about addressing the presence of DC components in the grid signal. Moreover, it is not immune to harmonics. These issues are considered in this work.

In this work, motivated by the results presented in [27], [35], [43], we propose a multiple circular limit cycle oscillator - frequency-locked loop (MCLO-FLL). The proposed MCLO-FLL can easily handle various disturbances commonly present in distorted grid *i.e.* harmonics, DC component *etc.* and discontinuous jumps in various grid voltage parameters. MCLO-FLL based three-phase sequences extraction technique is also presented. As the fundamental building block of the proposed technique uses nonlinear harmonic oscillator, it overcomes the problem of its linear counter part e.g. [26]. Linear oscillator [26] oscillates because the eigenvalues are $\pm i\omega$. In the presence of perturbation, the eigenvalues will no longer be purely imaginary conjugate, as a result oscillation will eventually die out. This is not the case for CLO. CLO is robustly stable i.e. the oscillation will not decay despite the presence of bounded disturbance. Moreover, the nonlinear structure also helps to get fast dynamic response. These are significant advantages of the MCLO-FLL over the existing literature.

The rest of the paper is organized as follows: The problem statement is given in Sec. II. Sec. III explains the proposed approach while dSPACE based hardware-in-the-loop (HIL) experimental results are given in Section IV. Finally, Section V concludes this paper.

II. Problem Statement

Single-phase grid voltage signal containing only the fundamental frequency is given by:

$$y = y_0 + A_g \sin\left(\underbrace{\omega_g t + \varphi}_{\theta}\right) \tag{1}$$

where $|y_0| \geq 0$ is the DC bias, A_g is the grid voltage amplitude, $f_g = \frac{\omega_g}{2\pi}$ is the frequency of the grid signal and $\theta \in [0, 2\pi)$ is the instantaneous phase angle. For the fundamental case, the problem is to estimate A_g, f_g and θ_g is the presence of various nonsmooth variations in phase, frequency, amplitude and DC bias.

In the presence of harmonic components, the single-phase grid voltage is given by:

$$y = y_0 + \sum_{i=1}^{n} A_{gi} \sin\left\{\underbrace{(2i-1)\,\omega_g t + \varphi_i}_{\theta_i}\right\} \tag{2}$$

where A_{gi} is the amplitude of the individual harmonic components, $f_{gi} = \frac{\omega_{gi}}{2\pi}$ is the frequency of the individual harmonic components and $\theta_i \in [0, 2\pi)$ is the instantaneous phase angle of the individual components. In this case, the problem is to estimate A_g, f_g and θ_g of the fundamental components despite the presence of harmonic components, DC bias and subject to various nonsmooth variations in phase, frequency, amplitude and DC bias. In the case of three-phase, in addition to the frequency estimation, estimating the positive, negative and zero sequences are also considered in this paper.

III. Proposed Approach

In this Section, first we recall the basics of the circular limit cycle oscillator (CLO) for the parameter estimation of single-phase grid voltage signal. Part of the results described in this Section originally appeared in [35], [45]. However, the model proposed in [35] can't handle the presence of DC bias and harmonics. In this work, we overcome the limitations of [35] by modifying the original structure. Moreover, application to three-phase case is also reported in this work

A. Basics of Circular Limit Cycle Oscillator

In the literature of nonlinear dynamical systems, second order nonlinear oscillatory systems are an important class of systems. They have been applied to solve many practical problems. Frequently this class of systems demonstrate an isolated trajectory in the phase plane (*i.e.* variable 1 vs. variable 2 plane). This kind of isolated trajectory is known as limit cycle and correspondingly an oscillator that has a limit cycle is known as limit cycle oscillator. Limit cycle can be of many shape. Circular limit cycle oscillator has a circularly shaped limit cycle. An advantage of this kind of limit cycle is that the shape is independent of the oscillator parameters or initial conditions. Motivated by the nonlinear dynamics literature, in this work we propose the following CLO which is a modified version of the oscillator given in Exercise 7.1.8 of [46]:

$$\dot{x}_1 = x_2\omega_n \tag{3a}$$
$$\dot{x}_2 = -x_1\omega_n - x_2\left(x_1^2 + x_2^2 - r^2\right) \tag{3b}$$

where x_1 and x_2 are the state variables, ω_n is the angular frequency of the sustained oscillation and r is the radius of the limit cycle in the x_1 vs. x_2 plane. The solutions of the CLO (3) are:

$$x_1(t) = -r\cos(\omega_n t),\, x_2(t) = r\sin(\omega_n t)$$

As the solution of $x_2(t)$ is similar to the grid voltage signal, CLO (3) can be considered as a proxy of the grid voltage signal. Then using proper feedback mechanism, any change in the grid voltage parameters, can be easily tracked using model (3).

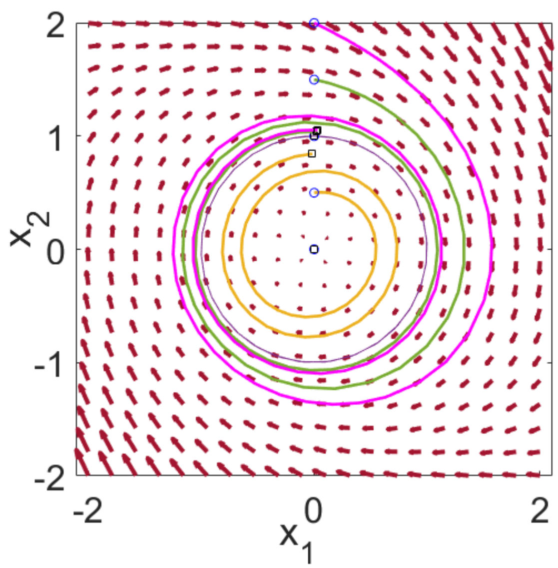

Figure 1. Phase portrait and numerical solution of the circular limit cycle oscillator (3) with $\omega = 2\pi$ and $r = 1$. In this figure $\rightarrow$ indicates the direction of the vector field, $\circ$ indicates the starting point *i.e.* initial condition and $\square$ indicates the final point of the solution.

A particular feature of CLO (3) is that it has an unstable equilibrium which is the origin and an almost globally asymptotically stable (A-GAS) limit cycle which is the circle of radius r denoted by $x_1^2 + x_2^2 = r^2$. It means, any trajectory that originates anywhere in the phase-plane, will converge to the circle of radius r except the one at origin. Fig. 1 shows the phase portrait of CLO. This Fig. shows that irrespective of the initial conditions, the trajectories converge to the unit circle. In addition to being A-GAS, the CLO is robust to bounded external disturbance/perturbation i.e. posses input-to-state stability (ISS) property. Using Lyapunov function based approach, these properties have been shown in [47, Proposition 5 and 6]. As such technical details are avoided here for the purpose of brevity. In this work, the focus is on the application aspect.

B. CLO based parameter estimation

Although CLO (3) can be considered as a model of the single-phase grid voltage signal, there are two limitations of this model. Firstly, CLO is not frequency adaptive. Secondly, in the presence of DC bias, grid signal is given by $y(t) = y_0 + A_g \sin(\omega_g t), y_0 > 0$, whereas for CLO the solution is $x_2(t) = r\sin(\omega_n t)$. So, steady-state error is inevitable. In order to tackle these problems, the following modification of CLO is proposed in this work:

$$\dot{x}_1 = x_2\omega \tag{4a}$$
$$\dot{x}_2 = \alpha(y - x_2 - x_4)\omega - x_1\omega - x_2\left(x_1^2 + x_2^2 - r^2\right) \tag{4b}$$
$$\dot{x}_3 = -\beta(y - x_2 - x_4)x_1\omega \tag{4c}$$
$$\dot{x}_4 = \gamma(y - x_2 - x_4) \tag{4d}$$

where $\alpha, \beta, \gamma > 0$ are the tuning parameters of the CLO, $\omega = \omega_n + 2\pi x_3$ is the estimated angular frequency with ω_n denoting the nominal grid frequency (in the steady-state $\omega = \omega_g$), r is the radius of CLO, x_4 represents the estimated value of the DC bias, $(y - x_2 - x_4)$ denotes the estimation error of the grid signal by the CLO and the phase angle dynamics of the grid voltage signal y is given by:

$$\dot{\theta}_g = -\omega_g \tag{5}$$

where θ_g and ω_g retain the same meaning as defined in Sec. II.

Remark 1. Eq. (4b), depends on the radius of the CLO which is also the amplitude of the grid voltage signal. However, estimating the amplitude adds computational complexity. To solve this problem, we have fixed $r = 1$ i.e. the nominal grid voltage amplitude. In non-nominal grid voltage condition, the oscillation amplitude of the CLO is no longer the same as the grid voltage amplitude from the theoretical point of view. However, in practice, even in non-ideal voltage condition, CLO continues to oscillate with the actual grid voltage amplitude (*cf.* Fig. 5a). As such setting $r = 1$ can be considered as an engineering solution to reduce the computational complexity of CLO.

Original CLO (3) oscillates at ω_n, however, the frequency adaptive CLO oscillates with the actual grid frequency ω_g, thanks to the feedback mechanism and the coupling of frequency adaptation part (4c). Due to the frequency adaptive nature of the CLO, for further analysis the modified CLO (4) is denoted as CLO- frequency-locked loop (CLO-FLL). In the steady state, $\alpha(y - x_2 - x_4)\omega \rightarrow 0$. Then the dynamics of eq. (4a) and (4b) are similar to the original CLO (3a) and (3b). As such the solutions are also similar *i.e.* $x_1(t) = -A_g\cos(\theta_g)$ and $x_2(t) = A_g\sin(\theta_g)$. Then the following formula gives the frequency, phase and amplitude of the actual grid signal y:

$$\omega_g = \omega_n + 2\pi x_3 \tag{6a}$$
$$\theta_g = \arctan\left\{x_2/\left(-x_1\right)\right\} \tag{6b}$$
$$A_g = \sqrt{x_1^2 + x_2^2} \tag{6c}$$

C. Stability analysis of CLO-FLL

This Section details the stability analysis of the CLO-FLL. For this purpose, we will use polar coordinate transformation. Prior to that, to couple the dynamics of the grid signal (5) into the CLO-FLL (4), let us introduce the instantaneous phase error as:

$$\Delta\theta = \theta - \theta_g \tag{7}$$

In polar coordinates, $x_1 = r\cos(\theta)$, $x_2 = r\sin(\theta)$ and $\theta = \arctan\left(x_2/x_1\right)$. To convert the dynamics from the Cartesian coordinates to polar coordinates, the following formulas are used [46]:

$$r\dot{r} = x_1\dot{x}_1 + x_2\dot{x}_2 \tag{8a}$$
$$\dot{\theta} = \left(x_1\dot{x}_2 - \dot{x}_1 x_2\right)/r^2 \tag{8b}$$

Using eq. (8a), the dynamics of the CLO-FLL (4a), (4b) can be written as:

$$\begin{aligned} r\dot{r} &= \alpha x_2\left(y - x_2 - x_4\right)\omega - x_2^2(x_1^2 + x_2^2 - 1) \\ &= \alpha e_{y-(x_2+x_4)} r\sin(\Delta\theta + \theta_g)\omega - r^2\sin^2(\Delta\theta + \theta_g) \\ \dot{r} &= \alpha e_{y-(x_2+x_4)}\sin(\Delta\theta + \theta_g)\omega - r\sin^2(\Delta\theta + \theta_g) \end{aligned} \tag{9}$$

where $e_{y-(x_2+x_4)} = A_g\sin(\theta_g) - r\sin(\Delta\theta + \theta_g) - x_4$. Using eq. (8b), the phase error dynamics can be written as:

$$\begin{aligned} \dot{\Delta\theta} &= \dot{\theta} - \dot{\theta}_g \\ &= \frac{x_1\dot{x}_2 - \dot{x}_1 x_2}{r^2} + \omega_g \\ &= \frac{-(x_1^2 + x_2^2)\omega - x_1x_2(x_1^2 + x_2^2 - 1)}{r^2} + \\ &\quad \frac{\alpha x_1(y - x_2 - x_4)\omega}{r^2} + \omega_g \\ \dot{\Delta\theta} &= \omega_g - \omega - \cos(\Delta\theta + \theta_g)\sin(\Delta\theta + \theta_g)(r^2 - 1) + \\ &\quad \frac{\alpha e_{y-(x_2+x_4)}\omega\cos(\Delta\theta + \theta_g)}{r} \end{aligned} \tag{10}$$

Then the overall closed-loop dynamics of the CLO-FLL (4) can be written as:

$$\dot{r} = \alpha e_{y-(x_2+x_4)}\sin(\Delta\theta + \theta_g)\omega - r\sin^2(\Delta\theta + \theta_g) \tag{11a}$$

$$\dot{\Delta\theta} = \omega_g - \omega - \cos(\Delta\theta + \theta_g)\sin(\Delta\theta + \theta_g)(r^2 - 1) + \frac{\alpha e_{y-(x_2+x_4)}\omega\cos(\Delta\theta + \theta_g)}{r} \tag{11b}$$

$$\dot{x}_3 = -\beta e_{y-(x_2+x_4)}\omega r\cos(\Delta\theta + \theta_g) \tag{11c}$$

$$\dot{x}_4 = \gamma e_{y-(x_2+x_4)} \tag{11d}$$

The desired equilibrium of eq. (11) is given by:

$$x^\star = \left\{r = A = A_g, \Delta\theta = 0, x_3 = \left(\omega_g - \omega_n\right)/2\pi, x_4 = y_o\right\} \tag{12}$$

Without losing any generality, for the sake of computational simplicity, we assume that $A_g = 1, y_o = 0.1$ The closed-loop dynamics (11) is nonlinear. However, we are interested in the local behavior of the closed-loop dynamics near the desired equilibrium given in eq. (12). This can be done by calculating the Jacobian matrix [48] of the system (11) near the desired equilibrium. The Jacobian matrix is given at the bottom of this page. Stability of the closed-loop dynamics near the equilibrium $x^\star$ is determined by the eigenvalues of the matrix $J(x^\star)$. This can be determined by the characteristics equation of the $J(x^\star)$ *i.e.* $\det(J(x^\star) - \lambda I_4) = 0$ which is given in the following:

$$c_4\lambda^4 + c_3\lambda^3 + c_2\lambda^2 + c_1\lambda + c_0\lambda^0 = 0 \tag{13}$$

where the coefficients are given by: $c_4 = 1$, $c_3 = \gamma + \alpha\omega_g + 2\sin^2(\theta_g)$, $c_2 = 2\gamma\sin^2(\theta_g) + 2\beta\pi\omega_g\{1 - \sin^2(\theta_g)\}$, $c_1 = 4\beta\pi\omega_g\left(\sin^2(\theta_g) - \sin^4(\theta_g)\right)$ and $c_0 = 0$. The stability of the polynomial (13) can be obtained through Routh-Hurwitz test. For this purpose, polynomial (13) can be rewritten as:

$$\lambda\left(c_4\lambda^3 + c_3\lambda^2 + c_2\lambda + c_1\right) = 0 \tag{14}$$

To show that the polynomial (14) doesn't have any roots in the right-half plane, let us consider the Routh-Hurwitz table given in Table I.

Since $1 - \sin^2(\theta_g) \geq 0, \forall\theta_g$ and $\sin^2(\theta_g) \geq \sin^4(\theta_g), \forall\theta_g$, then for suitably selected gain values, all the elements in the first column of the Routh-Hurwitz table are positive. This implies no sign change, as a result, no roots lie in the right-half plane. This together with the root at origin implies marginal stability of the closed-loop system. The root at origin is coming from the DC bias estimation loop given in Eq. (11d) which is a pure integrator. DC bias introduces steady-state error in the estimation. As such using a pure integrator to eliminate the steady-state error is a standard practice in the control system literature. Please consult [43] for detailed discussion on DC-bias estimation techniques in the context of grid synchronization techniques literature.

D. CLO-FLL parameters tuning

This section gives a guidelines on the tuning of the parameters α, β and γ of the CLO-FLL. For this purpose, we resort to the standard literature in linear control theory. For further development, assume that $\theta_g = 0$. This simplifies the polynomial (13) to

$$\begin{aligned} \lambda^4 + (\gamma + \alpha\omega_g)\lambda^3 + 2\pi\beta\omega_g\lambda^2 = 0 \\ \lambda^2 + (\gamma + \alpha\omega_g)\lambda^1 + 2\pi\beta\omega_g = 0 \end{aligned} \tag{15}$$

The denominator polynomial of a second-order transfer function is given by

$$\lambda^2 + 2\zeta\omega_0\lambda + \omega_0^2 = 0 \tag{16}$$

By comparing the eq. (15) to that of second-order transfer function's denominator polynomial (16), one can find that and $2\zeta\omega_o = \gamma + \alpha\omega_g$. If we choose the damping ratio to be $\zeta = \frac{1}{\sqrt{2}}$, then the following can be obtained:

$$\omega_o = \frac{1}{\sqrt{2}}(\gamma + \alpha\omega_g) \tag{17a}$$

$$\omega_o = \sqrt{2\pi\beta\omega_g} \tag{17b}$$

By solving the nonlinear equations (17a) and (17b), one can obtain that

$$J\left(x^\star\right) = \begin{bmatrix} (2 + \alpha\omega_g)\{\cos^2(\theta_g - 1)\} & -\alpha\omega_g\sin\left(2\theta_g\right)/2 & 0 & -\alpha\omega_g\sin\left(\theta_g\right) \\ -(2 + \alpha\omega_g)\sin\left(2\theta_g\right)/2 & -\alpha\omega_g\cos^2(\theta_g) & -2\pi & -\alpha\omega_g\cos\left(\theta_g\right) \\ \beta\omega_g\sin\left(2\theta_g\right)/2 & \beta\omega_g\cos^2(\theta_g) & 0 & \beta\omega_g\cos\left(\theta_g\right) \\ -\gamma\sin\left(\theta_g\right) & -\gamma\cos\left(\theta_g\right) & 0 & -\gamma \end{bmatrix}$$

Table I
ROUTH-HURWITZ TABLE

λ^3	1	$2\gamma\sin^2(\theta_g)+2\beta\pi\omega_g\{1-\sin^2(\theta_g)\}$
λ^2	$\gamma+\alpha\omega_g+2\sin^2(\theta_g)$	$4\beta\pi\omega_g\left(\sin^2(\theta_g)-\sin^4(\theta_g)\right)$
λ^1	$\frac{4\gamma\sin^4(\theta_g)+2\gamma^2\sin^2(\theta_g)+2\pi\beta\omega_g\gamma(1-\sin^2(\theta_g))+2\pi\alpha\beta\omega_g^2(1-\sin^2(\theta_g))+2\alpha\gamma\omega)+2\pi\alpha\gamma\omega_g\sin^2(\theta_g)}{\gamma+\alpha\omega_g+2\sin^2(\theta_g)}$	0
λ^0	$\frac{8\pi\beta\omega_g(\sin^2(\theta_g)-\sin^4(\theta_g))(2\gamma\sin^4(\theta_g)+\pi\beta\gamma\omega_g+\pi\alpha\beta\omega_g^2+\sin^2(\theta_g)(\gamma^2+\pi\alpha\beta\omega_g^2+\alpha\gamma\omega_g-\pi\beta\gamma\omega_g))}{4\gamma\sin^4(\theta_g)+2\pi\beta\gamma\omega_g+2\pi\alpha\beta\omega_g^2+\sin^2(\theta_g)(2\gamma^2-2\pi\alpha\beta\omega_g^2+2\alpha\gamma\omega_g-2\pi\beta\gamma\omega_g)}$	0

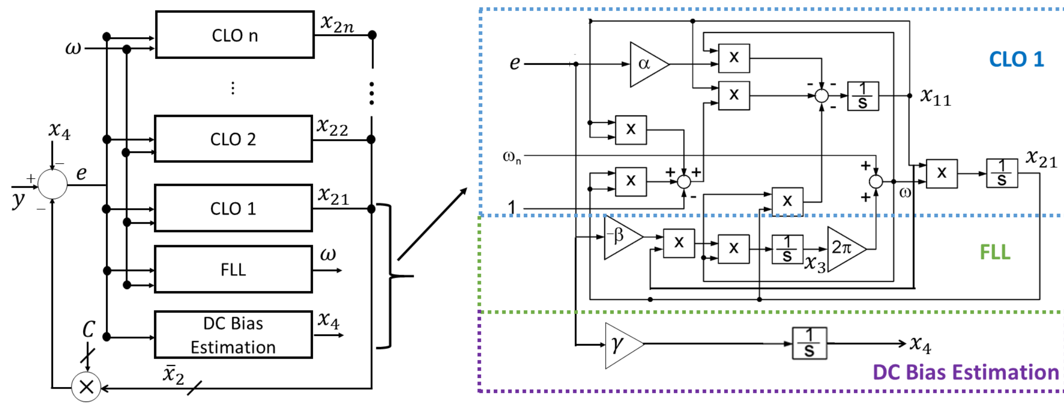

Figure 2. Block digram of the MCLO-FLL.

$$\alpha=\frac{\omega_0}{\sqrt{2}\omega_g},\beta=\frac{\omega_0^2}{2\pi\omega_g},\gamma=\frac{\omega_0}{\sqrt{2}} \quad (18)$$

Formula (18) can be considered as the starting point for tuning the gains of the CLO-FLL.

E. Extension and application of CLO-FLL to three-phase case

CLO-FLL proposed in Sec. III assumes that the grid signal is composed of a single frequency only with potentially subject to DC bias *i.e.* $y(t) = y_0 + A_g\sin(\omega_g t), y_0 > 0$. However, in practice, the presence of harmonics can't be neglected. Due to the modular nature of the CLO-FLL, by making multiple copies of CLO, it is possible to address the presence of harmonics. Following the ideas presented in [27], multi-frequency CLO-FLL (MCLO-FLL) can be implemented. Since the main idea is same as [27], details are avoided here for the purpose of brevity. Graphical representation of the MCLO-FLL is given in Fig. 2.

In addition to distorted single-phase grid, the proposed CLO-FLL can be directly applied to extract the sequences of the unbalanced and distorted three-phase grid voltage as well. Following the ideas presented in [30], CLO's can be used to generate the quadrature signals from the individual phase voltage signal. Then using the mathematical relationships given in eq. (7) and (8) of [30], the sequences of unbalanced grid can easily be estimated. Details are avoided here for the purpose brevity.

IV. EXPERIMENTAL RESULTS

In this Section, experimental results are considered using dSPACE 1104 board based hardware-in-the-loop (HIL) setup. The experimental setup used in this work is given in Fig. 3.

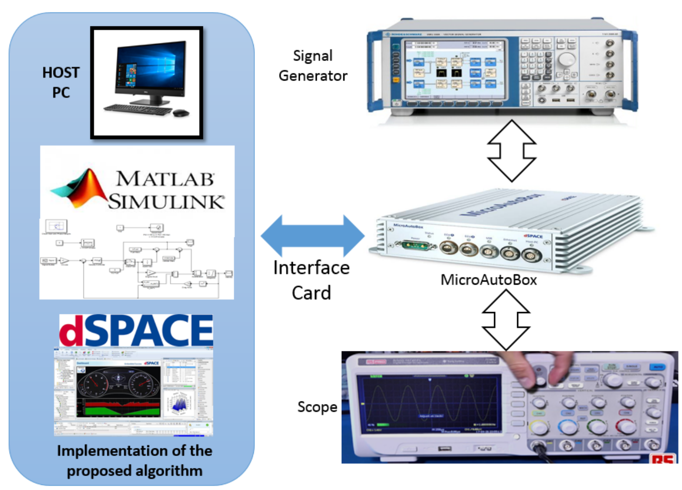

Figure 3. dSPACE-based HIL experimental system.

Using the third order Adams Bashforth scheme, the proposed MCLO-FLL technique was implemented in Simulink and the sampling frequency was 10KHz. Parameters of the MCLO-FLL are selected as $\alpha = 1/\sqrt{2}$, $\beta = 5$ and $\gamma = 80$. As a comparison tool, we have selected multiple EPLL (MEPLL) [42] and multiple SOGI-FLL (MSOGI-FLL) [27]. Both of these techniques in the standard form can't handle DC bias. So, we have modified them by following the guidelines given in [43]. Parameters of the EPLL are selected as $\mu_{1i} = \mu_{3i} = i \times \omega_n, i = 1, 3, 5, .., \mu_2 = 15000$ and $\mu_0 = 85$ with $\omega_n = 2\pi 50$. Parameters of the MSOGI-FLL are selected as: $k_0 = 0.25$, $k = \sqrt{2}$ and $\gamma = 50$. Both MEPLL and MSOGI-FLL are discretized using the third-order Adams Bashforth scheme for the sake of fair comparison.

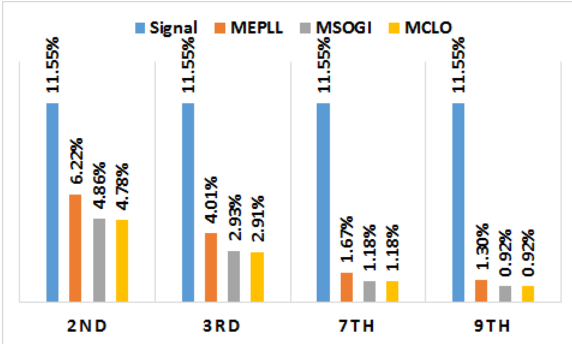

Figure 4. Harmonics robustness test summary.

A. Single-Phase case

For the experimental tests, we have considered a harmonic grid voltage signal with 20% total harmonic distortion (THD) comprised of 3^{rd}, 7^{th} and 9^{th} order harmonics each having 0.1155p.u. amplitude. In the first instant, we have used the test signal to check the harmonic robustness of the proposed technique *i.e.* when only one CLO-FLL block tuned at the fundamental frequency is considered. The result is summarized in Fig. 4. This result shows that MCLO-FLL produced the lowest THD among the comparison techniques. However, the THD is not zero. To obtain zero THD, multiple-filters approach *i.e.* MCLO-FLL is considered. Then to analyze the performances of the three-techniques, following step changes are considered as the test cases:

- Case 1: -0.2p.u. change in the fundamental amplitude
- Case 2: -0.15p.u. added as the DC component
- Case 3: $+5$Hz. change in the fundamental frequency
- Case 4: $+50^{\circ}$ change in the fundamental phase

Using the above test scenarios, the three techniques (MCLO-FLL, MEPLL and MSOGI-FLL) are then tested. Comparative experimental results are given in Fig. 5 and 6 respectively. Time domain performance summary of the three techniques can be found in Table II. These results demonstrate that the performance improvement by the proposed technique over state of the art techniques. MCLO-FLL performed better than the selected techniques in most of the cases. It has the lowest settling time for both phase and frequency. Similarly MCLO-FLL has the lowest frequency estimation overshoot among the comparison techniques. The only area where MCLO-FLL is not the absolute winner is the phase estimation error. However, the performance of MCLO-FLL in this regard is comparable with the comparison techniques. In terms of overall performance, MCLO-FLL can be considered as a potential tool to improve the performance of various power system monitoring and control applications.

B. Three-Phase case

As explained in Sec. III-E, MCLO-FLL is capable to extract the sequences of three-phase system. Parameters of MCLO-FLL are kept the same as in single-phase case. To test MCLO-FLL, an unbalanced and highly distorted grid signal is considered. The pre-fault value of the grid signal is considered as $\vec{V}_{pf} = 1\angle 0^{\circ}$. After the fault, harmonics, interharmonic and subharmonic are added to the grid voltage signal having a THD of 46%. Grid is polluted with $\vec{V}^{1}_{+} = 0.5\angle 0^{\circ}$, $\vec{V}^{1}_{-} = 0.25\angle 0^{\circ}$, $\vec{V}^{-}_{5} = 0.2\angle 0^{\circ}$, $\vec{V}^{+0}_{7} = 0.2\angle 0^{\circ}$and $\vec{V}^{0}_{11} = 0.2\angle 0^{\circ}$. In addition, sub harmonic of 20Hz. and interharmonic of 160Hz. are added with each having amplitude of 0.05p.u.Experimental results are given in Fig. 7. Experimental results demonstrate that MCLO-FLL successfully estimated the frequency and instantaneous components of the various sequences despite the grid signal being unbalanced and highly polluted. This demonstrate the suitability of MCLO-FLL for three-phase sequences extractions.

Table II
COMPARATIVE TIME DOMAIN PERFORMANCE SUMMARY.

	MCLO-FLL	MSOGI	MEPLL
-0.2p.u. amplitude change			
Settling time (± 0.1Hz.)	19ms	30ms	42ms
Settling time ($\pm 0.1^{\circ}$)	30ms	52ms	60ms
Frequency overshoot	0.3Hz.	0.32Hz.	0.45Hz.
Phase overshoot	2.65°	2.58°	3.85°
-0.1p.u. DC change			
Settling time (± 0.1Hz.)	19ms	20ms	21ms
Settling time ($\pm 0.1^{\circ}$)	48ms	48ms	35ms
Frequency overshoot	0.25Hz.	0.35Hz.	0.5Hz.
Phase overshoot	3.0°	2.2°	3.0°
$+5$Hz. freq. change			
Settling time (± 0.1Hz.)	50ms	72ms	57ms
Settling time ($\pm 0.1^{\circ}$)	62ms	92ms	90ms
Frequency overshoot	0Hz.	0.2Hz.	0.15Hz.
Phase overshoot	15.6°	16.2°	14.1°
$+50^{\circ}$ phase change			
Settling time (± 0.1Hz.)	60ms	85ms	58ms
Settling time ($\pm 0.1^{\circ}$)	76ms	108ms	106ms
Frequency overshoot	4.55Hz.	5.2Hz.	5.3Hz.
Phase overshoot	NA	NA	NA

*NA=Not Applicable

V. CONCLUSIONS

This paper demonstrated multiresonant nonlinear harmonic oscillators based estimation technique for single-phase and three-phase grid voltage signal. First a nonlinear oscillator is used as a model for the grid voltage signal. Then using standard results from the literature, some modifications are proposed to make the model frequency adaptive and DC bias robust. Using polar coordinate transformation and linearization, local stability analysis of the overall closed-loop system has been performed. Simple gain tuning rules are also provided. Comparative analysis with multiple EPLL and multiple SOGI-FLL based techniques have been performed using distorted grid voltage signals. Various step changes in parameters are performed to test the robustness of the different techniques. Experimental results demonstrated the superiority of the proposed technique.

Several future works are planned *e.g.* applying the MCLO-FLL as the frequency identifier block in proportional resonant (PR) controller based grid synchronization technique, grid friendly appliance controller, real time identification of transients and fluctuations in the context of future smart-grid. In this work, local stability analysis around the equilibrium point has been provided. As such quantifying the domain

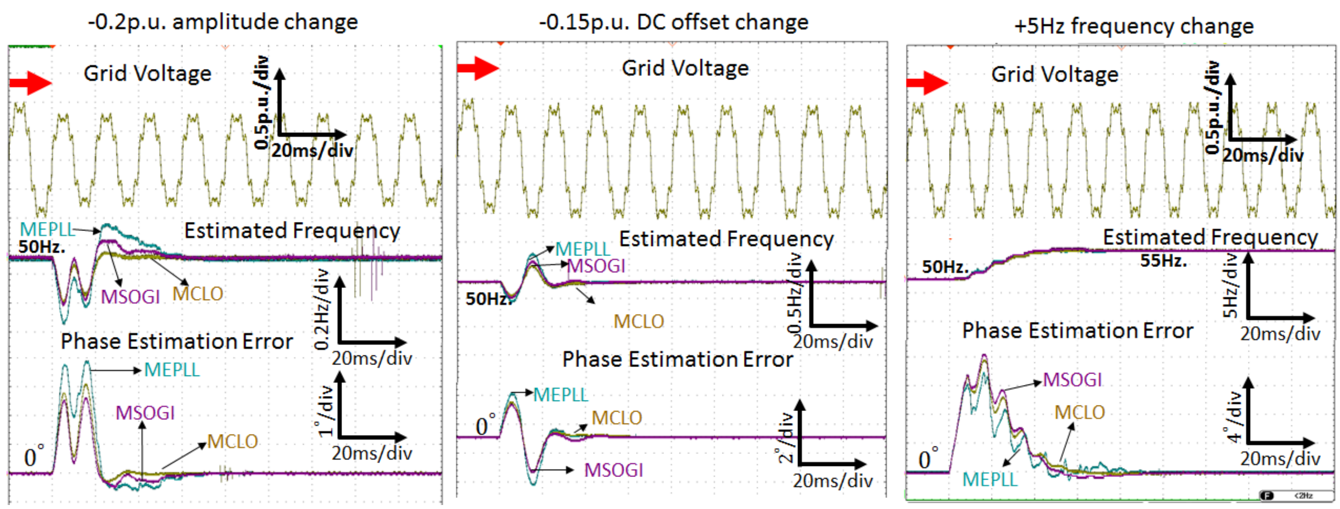

(a) Case 1 (b) Case 2 (c) Case 3

Figure 5. Experimental results (a) Case 1, (b) Case 2 and (c) Case 3.

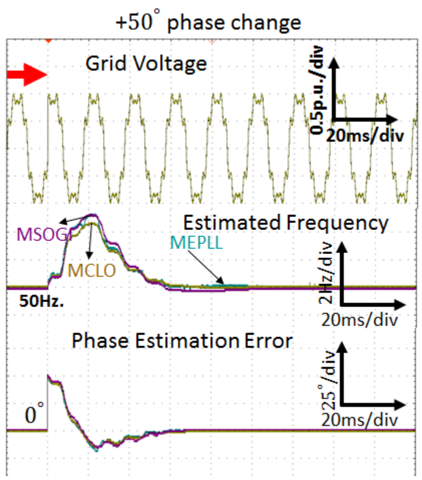

Figure 6. Experimental Results for Case 4.

of attraction (i.e. the set of all points that converge) for the equilibrium point could be interesting and will be considered in a future work.

REFERENCES

[1] B. Singh, P. Shah, and I. Hussain, "ISOGI-Q based control algorithm for single stage grid tied SPV system," *IEEE Transactions on Industry Applications*, vol. 54, no. 2, pp. 1136 – 1145, 2017.

[2] N. Panten, N. Hoffmann, and F. W. Fuchs, "Finite control set model predictive current control for grid-connected voltage-source converters with lcl filters: A study based on different state feedbacks," *IEEE Transactions on Power Electronics*, vol. 31, no. 7, pp. 5189–5200, 2016.

[3] X. Fu, S. Li, A. Hadi, and R. Challoo, "Novel neural control of single-phase grid-tied multilevel inverters for better harmonics reduction," *Electronics*, vol. 7, no. 7, p. 111, 2018.

[4] R. Kanagavel, V. Indragandhi, K. Palanisamy, and R. Kannan, "A novel current control technique for photo voltaic integrated single phase shunt active power filter," *International Journal of Renewable Energy Research (IJRER)*, vol. 7, no. 4, pp. 1709–1722, 2017.

[5] P. Acuna, L. Moran, M. Rivera, J. Dixon, and J. Rodriguez, "Improved active power filter performance for renewable power generation systems," *IEEE Transactions on Power Electronics*, vol. 29, no. 2, pp. 687–694, 2014.

[6] A. Micallef, "Review of the current challenges and methods to mitigate power quality issues in single-phase microgrids," *IET Generation, Transmission & Distribution*, vol. 13, no. 11, pp. 2044–2054, 2019.

[7] M. C. Kisacikoglu, M. Kesler, and L. M. Tolbert, "Single-phase on-board bidirectional PEV charger for V2G reactive power operation," *IEEE Transactions on Smart Grid*, vol. 6, no. 2, pp. 767–775, 2015.

[8] V. Monteiro, B. Exposto, J. C. Ferreira, and J. L. Afonso, "Improved vehicle-to-home (iV2H) operation mode: experimental analysis of the electric vehicle as off-line ups," *IEEE Transactions on Smart Grid*, vol. 8, no. 6, pp. 2702–2711, 2017.

[9] F. Blaabjerg, R. Teodorescu, M. Liserre, and A. V. Timbus, "Overview of control and grid synchronization for distributed power generation systems," *IEEE Transactions on Industrial Electronics*, vol. 53, no. 5, pp. 1398–1409, 2006.

[10] Z. Oubrahim, V. V. Choqueuse, Y. Amirat, and M. Benbouzid, "Maximum-likelihood frequency and phasor estimations for electric power grid monitoring," *IEEE Transactions on Industrial Informatics*, vol. 14, no. 1, pp. 167–177, 2018.

[11] H. Wen, C. Li, and W. Yao, "Power system frequency estimation of sine-wave corrupted with noise by windowed three-point interpolated dft," *IEEE Transactions on Smart Grid*, vol. 9, no. 5, pp. 5163–5172, 2018.

[12] M. S. Reza and V. G. Agelidis, "A robust technique for single-phase grid voltage fundamental and harmonic parameter estimation," *IEEE Transactions on Instrumentation and Measurement*, vol. 64, no. 12, pp. 3262–3273, 2015.

[13] S. Nanda and P. K. Dash, "A gauss–newton adaline for dynamic phasor estimation of power signals and its fpga implementation," *IEEE Transactions on Instrumentation and Measurement*, vol. 67, no. 1, pp. 45–56, 2018.

[14] H.-S. Song and K. Nam, "Instantaneous phase-angle estimation algorithm under unbalanced voltage-sag conditions," *IEE Proceedings-Generation, Transmission and Distribution*, vol. 147, no. 6, pp. 409–415, 2000.

[15] A. Vidal, F. D. Freijedo, A. G. Yepes, P. Fernandez-Comesaña, J. Malvar, O. Lopez, and J. Doval-Gandoy, "A fast, accurate and robust algorithm to detect fundamental and harmonic sequences," in *Energy Conversion Congress and Exposition (ECCE), 2010 IEEE*, pp. 1047–1052, IEEE, 2010.

[16] M. Beza and M. Bongiorno, "Application of recursive least squares algorithm with variable forgetting factor for frequency component estimation in a generic input signal," *IEEE Transactions on Industry Applications*, vol. 50, no. 2, pp. 1168–1176, 2014.

[17] P. Regulski and V. Terzija, "Estimation of frequency and fundamental power components using an unscented kalman filter," *IEEE Transactions on Instrumentation and Measurement*, vol. 61, no. 4, pp. 952–962, 2012.

[18] H. Ahmed, S.-A. Amamra, and I. Salgado, "Fast estimation of phase and frequency for single phase grid signal," *IEEE Transactions on Industrial Electronics*, vol. 66, pp. 6408–6411, Aug 2019.

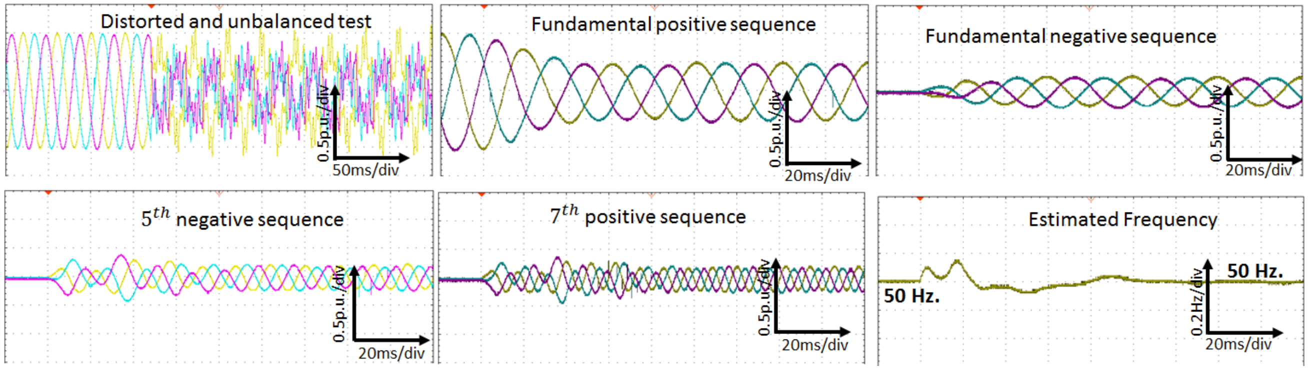

Figure 7. Experimental results for unbalanced distorted voltage test.

[19] R. Cardoso, R. F. de Camargo, H. Pinheiro, and H. A. Gründling, "Kalman filter based synchronisation methods," *IET generation, transmission & distribution*, vol. 2, no. 4, pp. 542–555, 2008.

[20] M. Karimi-Ghartemani, S. A. Khajehoddin, P. K. Jain, and A. Bakhshai, "Derivation and design of in-loop filters in phase-locked loop systems," *IEEE Transactions on Instrumentation and Measurement*, vol. 61, no. 4, pp. 930–940, 2012.

[21] M. Karimi-Ghartema, *Enhanced phase-locked loop structures for power and energy applications*. John Wiley & Sons, 2014.

[22] S. M. Silva, B. M. Lopes, R. P. Campana, W. Bosventura, *et al.*, "Performance evaluation of PLL algorithms for single-phase grid-connected systems," in *Industry Applications Conference, 2004. 39th IAS Annual Meeting. Conference Record of the 2004 IEEE*, vol. 4, pp. 2259–2263, IEEE, 2004.

[23] I. Carugati, P. Donato, S. Maestri, D. Carrica, and M. Benedetti, "Frequency adaptive PLL for polluted single-phase grids," *IEEE Transactions on Power Electronics*, vol. 27, no. 5, pp. 2396–2404, 2012.

[24] M. Bobrowska-Rafal, K. Rafal, M. Jasinski, and M. Kazmierkowski, "Grid synchronization and symmetrical components extraction with PLL algorithm for grid connected power electronic converters-a review," *Bulletin of the Polish Academy of Sciences: Technical Sciences*, vol. 59, no. 4, pp. 485–497, 2011.

[25] M. R. Amin and S. A. Zulkifli, "A framework for selection of grid-inverter synchronisation unit: Harmonics, phase-angle and frequency," *Renewable and Sustainable Energy Reviews*, vol. 78, pp. 210–219, 2017.

[26] F. D. Freijedo, A. G. Yepes, Ó. López, P. Fernandez-Comesana, and J. Doval-Gandoy, "An optimized implementation of phase locked loops for grid applications," *IEEE Transactions on Instrumentation and Measurement*, vol. 60, no. 9, pp. 3110–3119, 2011.

[27] P. Rodríguez, A. Luna, I. Candela, R. Mujal, R. Teodorescu, and F. Blaabjerg, "Multiresonant frequency-locked loop for grid synchronization of power converters under distorted grid conditions," *IEEE Transactions on Industrial Electronics*, vol. 58, no. 1, pp. 127–138, 2011.

[28] Z. D. Arani, S. A. Taher, A. Ghasemi, and M. Shahidehpour, "Application of multi-resonator notch frequency control for tracking the frequency in low inertia microgrids under distorted grid conditions," *IEEE Transactions on Smart Grid*, vol. 10, no. 1, pp. 337–349, 2019.

[29] A. B. Shitole, H. M. Suryawanshi, G. G. Talapur, S. Sathyan, M. S. Ballal, V. B. Borghate, M. R. Ramteke, and M. A. Chaudhari, "Grid interfaced distributed generation system with modified current control loop using adaptive synchronization technique," *IEEE Transactions on Industrial Informatics*, vol. 13, no. 5, pp. 2634–2644, 2017.

[30] D. Yazdani, M. Mojiri, A. Bakhshai, and G. Joos, "A fast and accurate synchronization technique for extraction of symmetrical components," *IEEE Transactions on Power Electronics*, vol. 24, no. 3, pp. 674–684, 2009.

[31] Y. Xia, S. Kanna, and D. P. Mandic, "Maximum likelihood parameter estimation of unbalanced three-phase power signals," *IEEE Transactions on Instrumentation and Measurement*, vol. 67, no. 3, pp. 569–581, 2018.

[32] V. Choqueuse, A. Belouchrani, F. Auger, and M. Benbouzid, "Frequency and phasor estimations in three-phase systems: Maximum likelihood algorithms and theoretical performance," *IEEE Transactions on Smart Grid*, pp. 1–1, 2018.

[33] Z. Oubrahim, V. V. Choqueuse, Y. Amirat, and M. Benbouzid, "Disturbances classification based on a model order selection method for power quality monitoring," *IEEE Transactions on Industrial Electronics*, vol. 64, no. 12, pp. 9421–9432, 2017.

[34] E. Oviedo, N. Vázquez, and R. Femat, "Synchronization technique of grid-connected power converters based on a limit cycle oscillator," *IEEE Transactions on Industrial Electronics*, vol. 65, no. 1, pp. 709–717, 2018.

[35] H. Ahmed, S.-A. Amamra, and M. Bierhoff, "Frequency-locked loop based estimation of single-phase grid voltage parameters," *IEEE Transactions on Industrial Electronics*, vol. 66, no. 11, pp. 8856–8859, 2019.

[36] M. L. Pay and H. Ahmed, "Modeling and tuning of circular limit cycle oscillator fll with pre-loop filter," *IEEE Transactions on Industrial Electronics*, 2019.

[37] F. Cupertino, E. Lavopa, P. Zanchetta, M. Sumner, and L. Salvatore, "Running DFT-based PLL algorithm for frequency, phase, and amplitude tracking in aircraft electrical systems," *IEEE Transactions on industrial Electronics*, vol. 58, no. 3, pp. 1027–1035, 2011.

[38] S. Golestan, M. Ramezani, J. M. Guerrero, F. D. Freijedo, and M. Monfared, "Moving average filter based phase-locked loops: Performance analysis and design guidelines," *IEEE Transactions on Power Electronics*, vol. 29, no. 6, pp. 2750–2763, 2014.

[39] K.-J. Lee, J.-P. Lee, D. Shin, D.-W. Yoo, and H.-J. Kim, "A novel grid synchronization pll method based on adaptive low-pass notch filter for grid-connected pcs," *IEEE transactions on industrial electronics*, vol. 61, no. 1, pp. 292–301, 2014.

[40] Q. Huang and K. Rajashekara, "An improved delayed signal cancellation pll for fast grid synchronization under distorted and unbalanced grid condition," *IEEE Transactions on Industry Applications*, vol. 53, no. 5, pp. 4985–4997, 2017.

[41] H. A. Hamed, A. F. Abdou, E. H. Bayoumi, and E. El-Kholy, "Frequency adaptive cdsc-pll using axis drift control under adverse grid condition," *IEEE Transactions on Industrial Electronics*, vol. 64, no. 4, pp. 2671–2682, 2017.

[42] M. Karimi-Ghartemani and M. R. Iravani, "Measurement of harmonics/inter-harmonics of time-varying frequencies," *IEEE Transactions on Power Delivery*, vol. 20, no. 1, pp. 23–31, 2005.

[43] M. Karimi-Ghartemani, S. A. Khajehoddin, P. K. Jain, A. Bakhshai, and M. Mojiri, "Addressing DC component in PLL and notch filter algorithms," *IEEE Transactions on Power Electronics*, vol. 27, no. 1, pp. 78–86, 2012.

[44] Y. Yang, L. Hadjidemetriou, F. Blaabjerg, and E. Kyriakides, "Benchmarking of phase locked loop based synchronization techniques for grid-connected inverter systems," *Proc. ICPE ECCE Asia*, pp. 2517–2524, 2015.

[45] H. Ahmed, R. Ushirobira, and D. Efimov, "Experimental study of the robust global synchronization of brockett oscillators," *The European Physical Journal Special Topics*, vol. 226, no. 15, pp. 3199–3210, 2017.

[46] S. H. Strogatz, *Nonlinear dynamics and chaos: with applications to physics, biology, chemistry, and engineering*. CRC Press, 2018.

[47] H. Ahmed, R. Ushirobira, and D. Efimov, "Robust global synchronization of brockett oscillators," *IEEE Transactions on Control of Network Systems*, vol. 6, pp. 289–298, March 2019.

[48] H. K. Khalil, *Nonlinear control*. Prentice Hall, 2014.

Hafiz Ahmed (S'10, M'17) received the B.Sc. degree in Electrical & Electronic Engineering from Ahsanullah University of Science and Technology, Dhaka, Bangladesh, in 2011, the M.Sc. degree in Systems, Control and Information Technology from Joseph Fourier University, Grenoble, France, in 2013, and the Ph.D. degree in Automatic Control from the University of Lille 1, France, in 2016.

For the Ph.D. thesis, he received the EECI (European Embedded Control Institute) Ph.D. award, 2017. He has also obtained the Best PhD Theses award from the Research Cluster on Modeling, Analysis and Management of Dynamic Systems (GDR-MACS) of the National Council of Scientific Research (CNRS) in France in 2017. He was a Postdoctoral fellow at Clemson University, SC, USA followed by academic appointments in Bangladesh at the University of Asia Pacific and North South University. Since September 2017, he joined the School of Mechanical, Aerospace and Automotive Engineering, Coventry University, United Kingdom. He is interested in applied control engineering with special focus in energy and environment. He is an Associate Editor of the INTERNATIONAL JOURNAL OF ELECTRICAL ENGINEERING & EDUCATION.

Michael Bierhoff (M'12) was born in Dortmund, Germany, in 1974. He received his Dipl.-Ing. (FH) degree in 2001 from the University of Applied Sciences, Dortmund, Germany, and the doctorate (Ph.D.) degree from the University of Kiel, Germany, in 2009.

From 2006 – 2011 he was with Still GmbH, Hamburg, Germany, as a research engineer. Since 2012 he has been a member of the faculty of Electrical Engineering and Computer Science of the University of Applied Sciences, Stralsund, Germany. His research interests include electrical drives and power electronics.

Mohamed Benbouzid (S'92–M'95–SM'98) received the B.Sc. degree in electrical engineering from the University of Batna, Batna, Algeria, in 1990, the M.Sc. and Ph.D. degrees in electrical and computer engineering from the National Polytechnic Institute of Grenoble, Grenoble, France, in 1991 and 1994, respectively, and the Habilitation à Diriger des Recherches degree from the University of Picardie "Jules Verne," Amiens, France, in 2000.

After receiving the Ph.D. degree, he joined the Professional Institute of Amiens, University of Picardie "Jules Verne," where he was an Associate Professor of electrical and computer engineering. Since September 2004, he has been with the University of Brest, Brest, France, where he is a Full Professor of electrical engineering. Prof. Benbouzid is also a Distinguished Professor and a 1000 Talent Expert at the Shanghai Maritime University, Shanghai, China. His main research interests and experience include analysis, design, and control of electric machines, variable-speed drives for traction, propulsion, and renewable energy applications, and fault diagnosis of electric machines.

Prof. Benbouzid is a Fellow of the IET and an IEEE Senior Member. He is the Editor-in-Chief of the INTERNATIONAL JOURNAL ON ENERGY CONVERSION. He is also an Associate Editor of the IEEE TRANSACTIONS ON ENERGY CONVERSION and the IEEE TRANSACTIONS ON VEHICULAR TECHNOLOGY. He is a Subject Editor for the IET RENEWABLE POWER GENERATION.